Published in final edited form as:
Anal Chem. 2011 January 1; 83(1): 207–215. doi:10.1021/ac102264z.

Mapping Lipid Alterations in Traumatically Injured Rat Spinal Cord by Desorption Electrospray Ionization Imaging Mass Spectrometry

Marion Girod[a], **Yunzhou Shi**[b], **Ji-Xin Cheng**[b,*], and **R. Graham Cooks**[a,*]

[a]Department of Chemistry and Center for Analytical Instrumentation Development, Purdue University, West Lafayette, IN 47907, USA

[b]Weldon School of Biomedical Engineering, Purdue University, West Lafayette, IN 47907, USA

Abstract

Desorption electrospray ionization (DESI) mass spectrometry is used in an imaging mode to interrogate the lipid profiles of 15 μm thin tissues cross sections of injured rat spinal cord and normal healthy tissue. Increased relative intensities of fatty acids, diacylglycerols and lysolipids (between +120% and +240%) as well as a small decrease in intensities of lipids (−30%) were visualized in the lesion epi-center and adjacent areas after spinal cord injury. This indicates the hydrolysis of lipids during the demyelination process due to activation of phospholipase A_2 enzyme. In addition, signals corresponding to oxidative degradation products, such as prostaglandin and hydroxyeicosatetraenoic acid, exhibited increased signal intensity by a factor of two in the negative ion mode in lesions relative to the normal healthy tissue. Analysis of malondialdehyde, a product of lipid peroxidation and marker of oxidative stress, was accomplished in the ambient environment using reactive DESI mass spectrometry imaging. This was achieved by electrospraying reagent solution containing dinitrophenylhydrazine as high velocity charged droplets onto the tissue section. The hydrazine reacts selectively and rapidly with the carbonyl groups of malondialdehyde and signal intensity of twice the intensity was detected in the lesions compared to healthy spinal cord. With a small amount of tissue sample, DESI-MS imaging provides information on the composition and distribution of specific compounds (limited by the occurrence of isomeric lipids with very similar fragmentation patterns) in lesions after spinal cord injury in comparison with normal healthy tissue allowing identification of the extent of the lesion and its repair.

Keywords

Desorption electrospray ionization; mass spectrometry; imaging; lipids; fatty acids; lipidomics; spinal cord injury

INTRODUCTION

Continued developments in imaging mass spectrometry (MS) have resulted in a variety of techniques to probe the spatial distribution of molecules within complex biological systems.[1, 2] Matrix-assisted laser desorption/ionization (MALDI) and secondary ion mass

*Corresponding Authors: R. Graham Cooks, Department of Chemistry, Purdue University, West Lafayette, IN 47907, USA, Tel: (765) 494-5262, Fax: (765) 494-9421, cooks@purdue.edu, Ji-Xin Cheng, Weldon School of Biomedical Engineering, Purdue University, West Lafayette, IN 47907, USA, Tel: (765) 494-4335, Fax: (765) 496-1912, jcheng@purdue.edu.

spectrometry (SIMS) imaging have been used extensively. MALDI imaging has been primarily applied to a variety of applications3–12 and can provide a spatial resolution of less than 100 μm13 but experiments are typically conducted under high vacuum and after application of an organic matrix to the sample to assist in ionization. Imaging using SIMS potentially provides the advantage of very high spatial resolution (ca.100 nm) and can be performed without additional sample preparation.14–21 However, SIMS imaging cannot be conducted under ambient conditions and is a harsher ionization technique that tends to produce more dissociation than MALDI. Desorption electrospray ionization (DESI) mass spectrometry22 was introduced as a method for the direct analysis of biological samples, including tissue sections. DESI offers the advantage of little or no sample preparation as it does not require the addition of matrix compounds and is conducted at atmospheric pressure under ambient conditions.22 Its disadvantages include a poorer spatial resolution than MALDI. It is one of a group of ambient ionization methods,23–25 amongst which the laser-based method of laser ablation electrospray ionization (LAESI)26–28 or laser ablation flowing atmospheric pressure afterglow (LA-FAPA)29 have give useful images of biological systems, including in vivo systems.

In DESI, a pneumatically-assisted electrospray produces charged droplets which are directed at the surface of the sample, creating a thin liquid film which dissolves the analytes.[30, 31] The impact of subsequent primary droplets releases secondary microdroplets containing analytes.[30, 31] This so-called ‘droplet pick-up’ process is followed by the standard electrospray evaporation mechanims which produce dry analyte ions.[32, 33] DESI has been used to construct chemical images of tissue sections[34–49] and in forensic analysis.[50, 51] The spatial resolution of DESI is typically 200 μm[36] although much better resolution of 100 μm has been reported.[37] Images showing the spatial distribution of particular compounds can provide chemical correlations with biological function or morphology. Recently, DESI-MS lipid imaging has also been reported as a potential diagnostic tool for disease detection including particular cancer and artheroma.[47, 52, 53]

Particular glycerophospholipids and their enzymatic products have been associated with malignant transformations in tissue.[54, 55] In other cases, the expression of phosphatidylserine in the outer leaflet of the membrane has been found to play a role in the recognition of altered cells, such as cancer cells, by macrophages.[56, 57] Lipids also play a role in artheroslerosis.[58–60] Change in the fatty acids and lipids composition has been reported in Alzeimer’s disease.[61, 62]

Lipids and fatty acids are the most common biomolecules found in the spinal cord and make up 50 % of its dry weight.63, [64] The crucial role of lipid oxidation and peroxidation through reactive oxygen species has been shown to be involved in the chemical processes associated with spinal cord injury (SCI).[65–70] Degenerative processes after SCI can be divided into a primary stage and a secondary stage.71 The initial mechanical insult by traction and compression forces breaks neuronal membranes. Beginning minutes to weeks after SCI, secondary destructive processes associated with the release of endogenous substances leads to inflammation, glutamate excitotoxicity, free radical release and ongoing demyelination and apoptosis of cells along the spinal cord. Multiple theories about secondary injury mechanisms have been developed over the last decade.[65–70, 72–75] Release of free fatty acids (FFAs), due to the activation of membrane phospholipases (PL) and lipases, is one of the first pathological events that follows primary trauma to the spinal cord.69, 70 FFAs are the components of membrane phospholipids having an important role in maintaining the structure and functions of the cell membranes. Severe impact SCI results in decreased total phospholipid content for up to 3 days following injury. Impact injury to spinal cord is associated with a biphasic increased in FFA level in spinal cord tissue. The first increase, observed within 5 min of spinal cord trauma, is followed by a decline 30 min after the

injury. The second increase, appearing 1 h after SCI, is more persistent. It peaks 24 h post trauma and declines over the following 6 days.[66, 69] Free arachidonic acid (AA, 20:4), due to the specific phospholipid composition of neurons, was reported to be the primary fatty acid released as a result of the injury-mediated tissue damage.[66] Plospholipase A_2 (PLA_2) and C are most likely to be responsible for liberation of FFAs from *sn-1* and *sn-2* positions, usually occupied by unsaturated fatty acids. Elevation of diacylglycerols (DG) and lysolipids levels have also been observed after compression of the spinal cord due to the lipids hydrolysis.[70] FFAs, and AA in particular, may lead to secondary damage to spinal cord neurons by including oxidative stress or increasing intercellular calcium level.76 Additionally, AA plays a significant role in the cell trauma by being the precursor of prostaglandin, thromboxane and leukotriene synthesis.77 It has been reported that experimental SCI induces significant production of eicosanoid compounds that can further contribute to secondary central nervous system injury.[78–80] Prostaglandins may also play a role in the complex biochemical mechanisms leading to vascular permeability and oedema formation.[81] The lipid and fatty acid peroxidation is catalyzed by free radical generated as a result of ischemic hypoxia and hemorrhage.[65, 72]

Due to the delayed nature of these events, the secondary phase of SCI is the most appropriate target stage for therapeutic intervention. Thus, a better understanding of the molecular mechanism of pathophysiology involved in tissue could open up new research possibilities and may lead to discovery of efficient therapies. This requires identifying the specific compounds involved but also requires determining where they are located in space and how they change in time. The main previous studies on altered lipid metabolism following spinal cord injury involved lipid and other compound extraction, which are then separated by liquid chromatography.[66, 70, 74] Information on the spatial distribution within the spinal cord is thus lost. Mechanical damages of the spinal cord after trauma can be visualized by magnetic resonance imaging (MRI)[82–85] or coherent anti-stokes Raman scattering (CARS)[86, 87] but without specific chemical information.

This work presents a study of traumatically injured rat spinal cord tissue sections analyzed by DESI imaging mass spectrometry. Injured and adjacent normal tissue sections were imaged and examined with DESI-MS in order to determine if differences were present in lipids profiles as determined by mass spectrometry and if so to characterize these differences and correlate them to the biochemical events associated with SCI. Tandem mass spectrometry (MS/MS) and exact mass measurements were used to identify the compounds detected. The aim was to determine whether DESI lipid imaging mass spectrometry has the potential to serve as a tool for detection of analyte changes in injured spinal cord samples.. An important note concerns the degree to which isomeric lipids can be characterized by imaging MS. Even with exact mass measurements, cases in which isomeric lipids occur will likely make MS/MS spectra difficult to interpret (or to distinguish in cases of a large number of isomers as is sometimes the case for natural lipids) and the assignment of compounds can be uncertain. This problem can be solved by extensive separation prior to MS analysis but such traditional experiments do not provide spatial distributions of compounds on anything like the scale of biological interest. When spatial distributions are essential, the structurally less specific imaging MS methods must be used, with appropriate caution

EXPERIMENTAL SECTION

Chemicals and Biological Samples

Methanol (MeOH) and dinitrophenylhydrazine (DNPH) were purchased from Sigma-Aldrich (St. Louis, MO, USA) and water (18.2 MΩ-cm) was from a PureLab ultra system by Elga LabWater (High Wycombe, UK). Adult male Long-Evans rats (Hilltop Lab Animals, Inc., Scottdale, Pennsylvania, USA) weighing 300–350 g were used.

Tissue Preparation

All protocols for this experiment were approved by the Purdue Animal Care and Use Committee. All rats were anesthetized deeply with the mixture of 90 mg/kg ketamine and 9 mg/kg xylazine. The tenth thoracic (T10) spine was removed by laminectomy. Contusion injury was performed with a New York University (NYU) weight-drop device under aseptic condition, dropping the 10-g rod (2.5 mm in diameter) on the exposed spinal cord surface from the height of 25 mm. After the contusion injury, the laminectomy was closed by suturing the muscle with 3-0 prolene followed by the use of 7.5 mm Michel wound clips (Fine Science Tools, Foster City, CA, USA) to close the skin incision. Animals were caged individually 1 week before the surgery and then up to 7 days post surgery. For post-operation pain management, the analgesics buprenorphine (0.05 mg/kg) were given every 12 h through subcutaneous injection during anesthesia recovery and for the first 3 days post surgery. At day 1 or day 7 post injury, animals were anesthetized (90 mg/kg ketamine and 9 mg/kg xylazine) and sacrificed by transcardial perfusion with cold PBS followed by 4% paraformaldehyde. Cord segments approximately 1 cm in length, both at the lesion epi-center and at least 3 cm rostral from the lesion, were extracted and stored at 4 °C until use. The spinal tissue about 1 cm long was cryostat-sectioned at 15 μm thickness and serially thaw mounted on slides. The slices were dried in the air under room temperature for 2 h, rehydrated in PBS solution for 15 min and washed once with PBS. Before imaging experiments, samples were dried under vacuum for 15 min.

Mass spectrometry

DESI imaging analysis were performed with a commercial Thermo Scientific LTQ (San Jose, CA, USA) linear ion trap mass spectrometer equipped with a custom-built, automated DESI source operated in both the negative and positive ion modes. The home-built DESI ion source is similar to the OmniSpray source from Prosolia Inc. (Indianapolis, IN, USA), configured as described previously.[88] A sprayer-to-surface distance of 2 mm, a spayer-to-inlet distance of 2.5 mm, an incident angle to the horizontal of 52° and a collection angle of 10° were used. The spray voltage was set at ± 5000 V and the capillary voltage at 5 V. Nitrogen gas was used as the nebulizing gas (140 psi). For the conventional DESI experiments, MeOH-water 50:50 (% v/v) was sprayed at a constant flow rate of 1.5 μL/min, while dinitrophenylhydrazine at 100 ppm was added in this solvent for the reactive DESI experiments. For the MS/MS experiments, a series of line scans across the tissue sample was performed during a period of about 1 min. An isolation window of 1.5 mass/charge units, a normalized collision energy of 20–40% (manufacturer's units) and a Mathieu parameter q_z value of 0.25 during collisional activation were used. Exact mass measurements were performed using a commercial Thermo Scientific LTQ-Orbitrap XL mass spectrometer (Bremen, Germany), with the resolution set to 100,000 to confirm molecular formulae. Mass standards were added into the DESI spray at a concentration of 10 ppm. The $[M-H]^-$ ion of taurocholate and $C_{15}H_{15}O_6N_3P_3F_{20}(C_2F_4)_2$ ultramark 1621 peak, with theoretical exact masses of 514.2839 and 1005.9727, respectively, were used as standards in the negative ion mode. The $[M+H]^+$ ion of reserpine and the $[M+Na]^+$ ion of cyclosporine A, theoretical exact masses of 609.2812 and 1224.3311, respectively, were used in the positive ion mode.[89]

In the imaging experiments, the tissue was scanned using a 2D moving stage (Newport, Richmond, CA, USA) in horizontal rows separated by a 150 μm vertical step until the entire tissue sample was analysed [43]. The lines were scanned at a constant velocity of 132 μm/s, while collecting one mass spectrum every 1.16 s over the range *m/z* 150–1000. The ion injection time was set to 500 ms and 5 microscans were averaged. Under these conditions, a lateral spatial resolution of ~ 200 μm can be achieved in DESI MS imaging.[36]

XCalibur 2.0 software (Thermo Scientific LTQ, San Jose, CA, USA) was used for instrument control, data acquisition and data processing. Lab-written software was used to convert the XCalibur mass spectra files (.raw) into a format compatible with BioMap. BioMap (freeware, http://www.maldi-msi.org/) was used to process the mass spectral data to generate two-dimensional ion images.

RESULTS AND DISCUSSION

Analysis of Lipids and Fatty Acids

Prior to the imaging experiments, DESI experimental conditions like geometrical parameters as well as electrospray parameters were optimized in order to maximize the signal intensity obtained from the thin tissue section, in particular for the lipid and fatty acid regions of the mass spectrum. A series of lines scans across the normal and injured tissue samples was performed and the mass spectra were examined. It is apparent from the line scans that differences in the mass spectrometric profiles exist between the normal and injured tissue types. Representative negative ion DESI mass spectra from direct analysis of rat spinal cord sections are shown in Figure 1. We note that in the positive ion mode, ions are only detected in the high *m/z* region (fatty acids are not easily ionized in the positive ion mode) with a lower signal/noise ratio[90] and no significant differences are observed between the injured and the normal tissue samples. The study therefore focused only on the negative ion mode. Glycerophospholipids and sphingolipids, as well as fatty acids are the main constituents detected in the negative ion mode in normal tissue (Figure 1a). In the low mass/charge region (*m/z* 200 – 400), ions corresponding to deprotonated free fatty acids are detected, while the region of *m/z* > 600 includes deprotonated forms of various lipids. As described in detail in a previous study,90 the lipid species detected from normal tissue sections of rat spinal cord mainly consist of sulfatides (ST), glycerophosphoserines (PS), glycerophosphoinositiols (PI), glycerophosphoethanolamines (PE) and plasmalogens (plasm-PE), glycerophosphoglycerols (PG) and, with lower intensity, glycerophosphocholines (PC) and sphingomyelin (SM). Confirmation of the lipid assignments was achieved by accurate mass measurements, tandem mass spectrometry (MS/MS) experiments, spectral comparisons with authentic lipid standards and comparisons to existing electrospray ionization (ESI) mass spectra.[91] A summary of the peak assignments and the relative abundances in the healthy spinal cord for negative ion $[M\text{-}H]^-$ ions can be found in a previous paper.[90]

In case of the injured sample (Figure 1b), in addition to the previously reported glycerophospholipids, sphingolipids and fatty acids, new compounds are detected both in the low mass/charge range and in the region from *m/z* 500 to *m/z* 650,. These ions have been identified based on the mass of the molecular anions and confirmation of the assignments was also achieved by tandem mass spectrometry (MS/MS) experiments and accurate mass measurements. The deprotonated form of arachidonic acid $[AA\text{-}H]^-$ is detected at *m/z* 303.4 (*m/z* 303.2307, error: −7.3 ppm using DESI on the Orbitrap). The molecular ion detected at *m/z* 335.4 has been identified as the deprotonated ion of 5,15-dihydroxyeicosanoic acid $[5,15\text{-diHETE-H}]^-$ (*m/z* 335.2271, error: +12.0 ppm on the DESI-Orbitrap) based on its MS/MS behavior[92] (Figure S1a in the Supporting Information). Fragmentation pathways supporting this identification are discussed in the Supporting Information. However, the MS/MS spectrum shown in Figure S1a slightly differs from published spectra[92] and could result of a mixture of diHETE's. Indeed, during the analysis of lipids directly in tissue, isobaric interferences can be observed in the CID experiments. The ion detected at *m/z* 353.4 in the MS spectrum of the injured specimen (Figure 1b) has been identified as the deprotonated prostaglandin $[F_{2\alpha}\text{-H}]^-$ (*m/z* 353.2354, error: +5.9 ppm on the DESI-Orbitrap). The MS/MS spectrum (Figure S1b in the Supporting Information) shows characteristic fragment ions from isoprostane compounds, and likely prostaglandin $F_{2\alpha}$.[93] However, isomeric

isoprostanes generated by radical-based oxidation of arachidonic acid may interfere. Returning to the mass spectrum, the ion detected at *m/z* 540.5 has been identified as hydrolyzed sulfatide [LysoST(18:1)-H]$^-$ on the basis of its accurate mass (*m/z* 540.2734, error: −18.5 ppm on the DESI-Orbitrap) and its MS/MS behavior (Figure S1c in the Supporting Information). The MS/MS spectrum of the ion detected at *m/z* 565.5 (*m/z* 565.4884, error: +8.1 ppm on the DESI-Orbitrap) allows this anion to be reasonably identified as the deprotonated diacylglycerol [DG(16:0/16:1)-H]$^-$ (Figure S1d in the Supporting Information).[94] Other diacylglycerol deprotonated ions can likewise be identified based on their CID spectra. Table 1 summarizes the main new compounds identified in the negative ion mode in the injured specimen using DESI-MS. We can note that even with high resolution measurement, the direct analysis of lipids in tissue without prior separation can suffer interferences in the MS/MS spectra due to isobaric compounds with the same elemental composition. Thus, the identification can be subject to uncertainly and LC/MS experiments could be done to isolate the compounds and confirm their assignments although with loss of the spatial information.

Tissue Imaging

Tissue imaging experiments allow increased information to gained from the line scans as well as the visualization of the results covering the entire tissue sample. Rat spinal cord cross sections were imaged using DESI-MS in the negative and the positive ion modes. Each ion image is a representation of the distribution of ions of one particular *m/z* value and hence a representation of the distribution of the corresponding molecule in the tissue sample. Note that the peak intensity does not exactly represent molecular concentrations in the tissue due to the differences in ionization efficiency, competitive suppression effects or differences in the degree of fragmentation. However, for the same molecule in the same tissue type or closely related compounds in the same tissue, relative peak intensities should approximately reflect differences in intrinsic concentrations. This is a standard assumption in imaging studies and it has been discussed and justified in previous papers.[34, 47, 48] To the extent that the assumption is justified, the chemical information obtained from the mass spectrometer can be correlated with the spatial information garnered from the images.

The spatial images of the normal and injured rat spinal cord tissue samples in the negative ion mode are shown in Figure 2. Each selected ion image is plotted on the same color scale to allow comparison of ion intensity between images. As seen in the images of injured samples, shown on the bottom of each images, the injured tissue exhibits increased absolute intensities for the signals at *m/z* 303.4, 335.4, 353.4, 540.5 and 565.5 when compared with normal tissue. Following the observations initially made with the DESI data from the line scans, the DESI-MS images allow the spatial localization of the injured site. The image of the ion detected at *m/z* 303.4, identified as the deprotonated form of arachidonic acid (AA), shows a much higher signal in the injured sample, and specially in the dorsal area (Figure 2b). A similar spatial intensity distribution is observed for ions reasonably assigned to deprotonated LysoST(18:1) and DG(32:1) detected at *m/z* 540.5 and 565.5, respectively (Figure 2e and f). In a complementary fashion, a small decrease of the ST(24:1) signal intensity, mainly located in the area corresponding to the white matter with less abundance in the gray matter in the normal spinal cord tissue,[90] is observed in the injured sample (Figure 2a). The species resulting from the hydrolysis of phospholipids, due to the production of enzyme PLA_2 during the SCI, can still be detected in the samples one week after the injury. This result slightly differs from the literature where the increase of FFAs and DG is followed by a decline around 10h after the SCI, even if time points later than 24h were not studied.[69, 70, 73, 74] However, a recent MALDI mass spectrometry imaging study has revealed the production of lysophosphatidylcholine in the injured ischemic rat brain 48h after the MCA occlusion.[95] In addition, signals at *m/z* 335.4 (Figure 2c) and *m/z* 353.4

(Figure 2d), which correspond to the deprotonated form of diHETE and $PGF2_{\alpha}$ are more intense in the injured spinal cord sample. This is ascribed to the peroxidation of AA occurring in the secondary phase of the spinal cord injury process. Changes of signal intensities are observed specifically in the dorsal area of the injured sample, corresponding to the gray matter. This is in agreement with a reported study[70] which suggests that the initial alteration in spinal cord lipid metabolism after trauma was in the gray matter and spread slowly into the white matter.[70]

Reactive DESI for Imaging of Malondialdehyde

The detection of eicosanoid compounds in the injured samples reveals lipid peroxidation. The marker malondialdehyde (MDA) is also widely used to assess the peroxidation processes. This aldehyde is produced by the radical breakdown of hydroperoxides resulting from lipids and fatty acids peroxidation containing at least two double bonds.[65, 67, 96] In order to be able to detect this low mass compound, reactive DESI experiments were done. This variant on the basic DESI experiment implements rapid chemical reactions occurring at the spot being sampled concurrently with acquisition of mass spectra to improve sensitivity and selectivity of detection of target molecules.[46, 97] The experiment is carry out by dissolving a suitable chemical reagent into the spray solvent; no sample preparation is needed. The quantitative method most frequently used for measuring low molecular mass carbonyl compounds such as aldehydes is based on derivatization with dinitrophenylhydrazine (DNPH) typically before liquid chromatography-tandem mass spectrometry coupling analysis.[98–101] Thus, DNPH was chosen as the reagent for improved sensitivity of carbonyl detection in negative ion mode mass spectrometry. The results show that the amino group of DNPH reacts selectively and rapidly with the two ketone groups of MDA (Scheme 1) to form the dihydrazone MDA.diDNPH product which is detected as a deprotonated ion at *m/z* 431.5 in the injured sample (Figure 3b). Confirmation of the assignments was achieved by tandem mass spectrometry (MS/MS) experiments and high resolution MS on the Orbitrap after exposure. The peak at *m/z* 431.0712 can be accurately assigned as having the exact mass of $[MDA.diDNPH\text{-}H]^-$ with an error of −4.4 ppm. Moreover, the MS/MS spectrum of dihydrazone $[MDA.diDNPH\text{-}H]^-$ (Figure S2 in the Supporting Inforamation) shows characteristic dissociation behavior.[100] The image of the peak at *m/z* 431.5 (Figure 4), extracted from the full set of data, shows the expected increased concentration in the dorsal area of the injured sample compared to the normal sample, even if the level of MDA is supposed to decrease few days after the SCI.[65, 67]

Reproducibility

Reproducibility is crucial to establish a potential method for distinguishing between normal and injured tissue samples. In this case, three different tissue samples from three different rats were analyzed, sufficient for initial experiments used to identify trends in the lipid species observed. Figure S3 in the Supporting Information shows the ratios of signal intensities of AA (*m/z* 303), diHETE (*m/z* 335), $PGF_{2\alpha}$ (*m/z* 353), LysoST(18:1) (*m/z* 540), DG(32:1) (*m/z* 565), ST(24:1) (*m/z* 888) and MDA diDNPH (*m/z* 431) between the injured and the normal tissues (I_{inj}/I_{nor}) for the three rats with a relative standard deviation less than 15%. The DESI-MS imaging method described here for lipid and fatty acid species in injured rat spinal cord has been demonstrated to be reproducible across multiple rats and within multiple samples from the same rat, yielding positive injury correlations.

CONCLUSION

It has been demonstrated that DESI-MS imaging can distinguish between normal and injured rat spinal cord tissue samples in the small set of tissue sections examined. The resulting ion images reflect the relative concentrations of the species detected from the tissue

surface. The data indicate hydrolysis of lipids during the demyelination process due to activation of phospholipase A_2 enzyme. In addition, oxidative degradation products, such as prostaglandin and HETE, exhibited increased signal intensity in the negative ion mode in lesions relative to the normal healthy spinal cords. The distinction between diseased and healthy tissue was made using multiple diacylglycerols and lysolipids as well as oxidative degradation products.

DESI imaging MS presents advantages in terms of easy implementation and ambient analysis. We note, however, that even with high resolution measurement, the direct analysis of lipids in tissue without prior separation can yield non-unique MS/MS spectra due to isomeric compounds which have the same elemental composition and similar fragmentation behavior. In such cases, explicit lipid identification can be subject to uncertainly, especially if mixtures of lipids are generated. Such difficulties can in principle be resolved by LC/MS experiments but only at the sacrifice of the imaging capability.

Reactive DESI has been implemented in order to directly detect the low molecular mass oxidative stress marker to increase confidence in the conclusions of the MS/MS experiments in revealing the identities of individual compounds. With this caveat, DESI-MS imaging therefore provides chemical and spatial information that contributes to a better understanding of lipid biochemistry during spinal cord injury. It may help in the development of drug treatment for injury recovery.

Supplementary Material

Refer to Web version on PubMed Central for supplementary material.

Acknowledgments

This work was supported by the U.S. National Institutes of Health (Grant 1R21EB009459-01).

REFERENCES

1. McDonnell LA, Heeren RMA. Mass Spectrometry Reviews 2007;26:606–643. [PubMed: 17471576]
2. Pacholski ML, Winograd N. Chemical Reviews 1999;99 2977-+
3. Andersson M, Groseclose MR, Deutch AY, Caprioli RM. Nature Methods 2008;5:101–108. [PubMed: 18165806]
4. Burnum KE, Frappier SL, Caprioli RM. Annual Review of Analytical Chemistry 2008;1:689–705.
5. Caprioli RM. Proteomics 2008;8:3679–3680. [PubMed: 18780396]
6. Francese S, Dani FR, Traldi P, Mastrobuoni G, Pieraccini G, Moneti G. Combinatorial Chemistry & High Throughput Screening 2009;12:156–174. [PubMed: 19199884]
7. Jackson SN, Woods AS. Journal of Chromatography B-Analytical Technologies in the Biomedical and Life Sciences 2009;877:2822–2829.
8. Landgraf RR, Conaway MCP, Garrett TJ, Stacpoole PW, Yost RA. Analytical Chemistry 2009;81:8488–8495. [PubMed: 19751051]
9. Roy S, Touboul D, Brunelle A, Germain DP, Laprevote O, Chaminade P. MS-Medecine Sciences 2005;21:55–56.
10. Sebastian M, Touboul D, Brunelle A, Laprevote O, Egido J, Vivanco F. Molecular & Cellular Proteomics 2005;4:S163–S163.
11. Seeley EH, Caprioli RM. Proceedings of the National Academy of Sciences of the United States of America 2008;105:18126–18131. [PubMed: 18776051]
12. Wolstenholme R, Bradshaw R, Clench MR, Francese S. Rapid Commun Mass Spectrom 2009;23:3031–3039. [PubMed: 19711300]

13. Stoeckli M, Chaurand P, Hallahan DE, Caprioli RM. Nature Medicine 2001;7:493–496.
14. Brunelle A, Touboul D, Laprevote O. Journal of Mass Spectrometry 2005;40:985–999. [PubMed: 16106340]
15. Magnusson Y, Friberg P, Sjovall P, Dangardt F, Malmberg P, Chen Y. Clinical Physiology and Functional Imaging 2008;28:202–209. [PubMed: 18363737]
16. Sjovall P, Lausmaa J, Johansson B. Analytical Chemistry 2004;76:4271–4278. [PubMed: 15283560]
17. Touboul D, Brunelle A, Halgand F, De La Porte S, Laprevote O. Journal of Lipid Research 2005;46:1388–1395. [PubMed: 15834124]
18. Touboul D, Kollmer F, Niehuis E, Brunelle A, Laprevote O. Journal of the American Society for Mass Spectrometry 2005;16:1608–1618. [PubMed: 16112869]
19. Sjovall P, Johansson B, Belazi D, Stenvinkel P, Lindholm B, Lausmaa J, Schalling M. Applied Surface Science 2008;255:1177–1180.
20. Gunnarsson A, Kollmer F, Sohn S, Hook F, Sjovall P. Analytical Chemistry 2010;82:2426–2433. [PubMed: 20163177]
21. Seyer A, Einhorn J, Brunelle A, Laprévote O. Analytical Chemistry 2010;82:2326–2333. [PubMed: 20155940]
22. Takats Z, Wiseman JM, Gologan B, Cooks RG. Science 2004;306:471–473. [PubMed: 15486296]
23. Sampson JS, Hawkridge AM, Muddiman DC. Journal of the American Society for Mass Spectrometry 2006;17:1712–1716. [PubMed: 16952462]
24. Sampson JS, Muddiman DC. Rapid Communications in Mass Spectrometry 2009;23:1989–1992. [PubMed: 19504481]
25. Brady JJ, Judge EJ, Levis RJ. Rapid Communications in Mass Spectrometry 2009;23:3151–3157. [PubMed: 19714710]
26. Nemes P, Barton AA, Li Y, Vertes A. Analytical Chemistry 2008;80:4575–4582. [PubMed: 18473485]
27. Nemes P, Barton AA, Vertes A. Analytical Chemistry 2009;81:6668–6675. [PubMed: 19572562]
28. Nemes P, Woods AS, Vertes A. Analytical Chemistry 2010;82:982–988. [PubMed: 20050678]
29. Shelley JT, Ray SJ, Hieftje GM. Analytical Chemistry 2008;80:8308–8313. [PubMed: 18826246]
30. Costa AB, Cooks RG. Chemical Physics Letters 2008;464:1–8.
31. Venter A, Sojka PE, Cooks RG. Analytical Chemistry 2006;78:8549–8555. [PubMed: 17165852]
32. Dole M, Mack LL, Hines RL. Journal of Chemical Physics 1968;49 2240-&.
33. Iribarne JV, Thomson BA. Journal of Chemical Physics 1976;64:2287–2294.
34. Dill AL, Ifa DR, Manicke NE, Zheng OY, Cooks RG. Journal of Chromatography B-Analytical Technologies in the Biomedical and Life Sciences 2009;877:2883–2889.
35. Esquenazi E, Dorrestein PC, Gerwick WH. Proceedings of the National Academy of Sciences of the United States of America 2009;106:7269–7270. [PubMed: 19416917]
36. Ifa DR, Wiseman JM, Song QY, Cooks RG. International Journal of Mass Spectrometry 2007;259:8–15.
37. Kertesz V, Van Berkel GJ. Rapid Communications in Mass Spectrometry 2008;22:2639–2644. [PubMed: 18666197]
38. Kertesz V, van Berkel GJ. Analytical Chemistry 2008;80:1027–1032. [PubMed: 18193892]
39. Kertesz V, Van Berkel GJ, Vavrek M, Koeplinger KA, Schneider BB, Covey TR. Analytical Chemistry 2008;80:5168–5177. [PubMed: 18481874]
40. Lane AL, Nyadong L, Galhena AS, Shearer TL, Stout EP, Parry RM, Kwasnik M, Wang MD, Hay ME, Fernandez FM, Kubanek J. Proceedings of the National Academy of Sciences of the United States of America 2009;106:7314–7319. [PubMed: 19366672]
41. Talaty N, Takats Z, Cooks RG. Analyst 2005;130:1624–1633. [PubMed: 16284661]
42. Wiseman JM, Ifa DR, Song QY, Cooks RG. Angewandte Chemie-International Edition 2006;45:7188–7192.
43. Wiseman JM, Ifa DR, Venter A, Cooks RG. Nature Protocols 2008;3:517–524.

44. Wiseman JM, Ifa DR, Zhu YX, Kissinger CB, Manicke NE, Kissinger PT, Cooks RG. Proceedings of the National Academy of Sciences of the United States of America 2008;105:18120–18125. [PubMed: 18697929]
45. Wiseman JM, Puolitaival SM, Takats Z, Cooks RG, Caprioli RM. Angewandte Chemie-International Edition 2005;44:7094–7097.
46. Wu CP, Ifa DR, Manicke NE, Cooks RG. Analytical Chemistry 2009;81:7618–7624. [PubMed: 19746995]
47. Manicke NE, Nefliu M, Wu C, Woods JW, Reiser V, Hendrickson RC, Cooks RG. Anal Chem 2009;81:8702–8707. [PubMed: 19803494]
48. Wu CP, Ifa DR, Manicke NE, Cooks RG. Analyst 2010;135:28–32. [PubMed: 20024177]
49. Eberlin LS, Ifa DR, Wu C, Cooks RG. Angewandte Chemie-International Edition 2009;49:873–876.
50. Ifa DR, Gumaelius LM, Eberlin LS, Manicke NE, Cooks RG. Analyst 2007;132:461–467. [PubMed: 17471393]
51. Ifa DR, Manicke NE, Dill AL, Cooks G. Science 2008;321:805–805. [PubMed: 18687956]
52. Dill AL, Ifa DR, Manicke NE, Costa AB, Ramos-Vara JA, Knapp DW, Cooks RG. Analytical Chemistry 2009;81:8758–8764. [PubMed: 19810710]
53. Eberlin LS, Dill AL, Costa AB, Ifa DR, Cheng L, Masterson T, Koch M, Ratliff TL, Cooks RG. Analytical Chemistry 2009;82:3430–3434. [PubMed: 20373810]
54. Glunde K, Jie C, Bhujwalla ZM. Cancer Research 2004;64:4270–4276. [PubMed: 15205341]
55. Aboagye EO, Bhujwalla ZM. Cancer Research 1999;59:80–84. [PubMed: 9892190]
56. Zwaal RFA, Comfurius P, Bevers EM. Cellular and Molecular Life Sciences 2005;62:971–988. [PubMed: 15761668]
57. Utsugi T, Schroit AJ, Connor J, Bucana CD, Fidler IJ. Cancer Research 1991;51:3062–3066. [PubMed: 2032247]
58. Morrow JD. Arteriosclerosis Thrombosis and Vascular Biology 2005;25:279–286.
59. Polidori MC, Pratico D, Savino K, Rokach J, Stahl W, Mecocci P. Journal of Cardiac Failure 2004;10:334–338. [PubMed: 15309701]
60. Pratico D, Iuliano L, Mauriello A, Spagnoli L, Lawson JA, Maclouf J, Violi F, FitzGerald GA. Journal of Clinical Investigation 1997;100:2028–2034. [PubMed: 9329967]
61. Montine TJ, Neely MD, Quinn JF, Beal MF, Markesbery WR, Roberts LJ, Morrow JD. Free Radical Biology and Medicine 2002;33:620–626. [PubMed: 12208348]
62. Söderberg M, Edlund C, Kristensson K, Dallner G. Lipids 1991;26:421–425. [PubMed: 1881238]
63. Agranoff, BW.; Binjamins, JA.; Hajra, AK. Basic Neurochmistry: Molecular, Cellular and Medical Aspects, 6th Ed. Sigel, GJ., et al., editors. Philadelphia: Lippincott Williams & Wilkins; 1999.
64. Morell, P.; Quarles, RH.; Norton, WT. Basic Neurochmistry: Molecular, Cellular and Medical Aspects, 5th Ed. Sigel, GJ., et al., editors. New York: Raven Press, Ltd.; 1994.
65. Kaynar MY, Hanci M, Kafadar A, Gumustas K, Belce A, Ciplak N. Neurosurgical Review 1998;21:117–120. [PubMed: 9795945]
66. Murphy EJ, Behrmann D, Bates CM, Horrocks LA. Molecular and Chemical Neuropathology 1994;23:13–26. [PubMed: 7893328]
67. Barut S, Canbolat A, Bilge T, Aydin Y, Cokneseli B, Kaya U. Neurosurgical Review 1993;16:53–59. [PubMed: 8483520]
68. Saunders RD, Dugan LL, Demediuk P, Means ED, Horrocks LA, Anderson DK. Journal of Neurochemistry 1987;49:24–31. [PubMed: 3108455]
69. Demediuk P, Saunders RD, Clendenon NR, Means ED, Anderson DK, Horrocks LA. Progress in Brain Research 1985;63:211–226. [PubMed: 2940621]
70. Demediuk P, Saunders RD, Anderson DK, Means ED, Horrocks LA. Proceedings of the National Academy of Sciences of the United States of America 1985;82:7071–7075. [PubMed: 3863139]
71. McDonald JW, Sadowsky C. Lancet 2002;359:417–425. [PubMed: 11844532]
72. Klussmann S, Martin-Villalba A. Journal of Molecular Medicine-Jmm 2005;83:657–671.

73. Pantovic R, Draganic P, Erakovic V, Blagovic B, Milin C, Simonic A. Spinal Cord 2005;43:519–526. [PubMed: 15852057]
74. Faden AI, Chan PH, Longar S. Journal of Neurochemistry 1987;48:1809–1816. [PubMed: 3033150]
75. Demediuk P, Saunders RD, Dugan LL, Anderson DK, Horrocks LA. Journal of Neurochemistry 1985;44:S50.
76. Toborek M, Malecki A, Garrido R, Mattson MP, Hennig B, Young B. Journal of Neurochemistry 1999;73:684–692. [PubMed: 10428065]
77. Bazan NG, Deturco EBR, Allan G. Journal of Neurotrauma 1995;12:791–814. [PubMed: 8594208]
78. Moreland DB, Soloniuk DS, Feldman MJ. Surgical Neurology 1989;31:277–280. [PubMed: 2928921]
79. Hsu CY, Halushka PV, Hogan EL, Cox RD. Journal of the Neurological Sciences 1986;74:289–296. [PubMed: 3525758]
80. Jonsson HT, Daniell HB. Prostaglandins 1976;11:51–61. [PubMed: 1257498]
81. Olsson Y, Sharma HS, Pettersson A, Cervosnavarro J. Circumventricular Organs and Brain Fluid Environment : Molecular and Functional Aspects 1992;91:197–203.
82. Sheikh KA. Experimental Neurology 2010;223:72–76. [PubMed: 19616546]
83. Goldberg AL, Kershah SM. Journal of Spinal Cord Medicine 2010;33:105–116. [PubMed: 20486529]
84. Shabshin N, Ougortsin V, Zoizner G, Gefen A. Clinical Biomechanics 2010;25:402–408. [PubMed: 20188448]
85. Martirosyan NL, Bennett KM, Theodore N, Preul MC. Neurosurgery 2010;66:131–136. [PubMed: 20023543]
86. Ouyang H, Sun WJ, Fu Y, Li JM, Cheng JX, Nauman E, Shi RY. Journal of Neurotrauma 2010;27:1109–1120. [PubMed: 20373847]
87. Wang HF, Fu Y, Zickmund P, Shi RY, Cheng JX. Biophysical Journal 2005;89:581–591. [PubMed: 15834003]
88. Manicke NE, Kistler T, Ifa DR, Cooks RG, Ouyang Z. Journal of the American Society for Mass Spectrometry 2009;20:321–325. [PubMed: 19013081]
89. Manicke NE, Dill AL, Ifa DR, Cooks RG. J Mass Spectrom 45:223–226. [PubMed: 20049747]
90. Girod M, Shi Y, Cheng JX, Cooks RG. Journal of the American Society for Mass Spectrometry 2010;21:1177–1189. [PubMed: 20427200]
91. Pulfer M, Murphy RC. Mass Spectrometry Reviews 2003;22:332–364. [PubMed: 12949918]
92. Wheelan P, Zirrolli JA, Murphy RC. Journal of the American Society for Mass Spectrometry 1996;7:140–149.
93. Murphy RC, Barkley RM, Berry KZ, Hankin J, Harrison K, Johnson C, Krank J, McAnoy A, Uhlson C, Zarini S. Analytical Biochemistry 2005;346:1–42. [PubMed: 15961057]
94. Leikera TJ, Barkleya RM, Murphy RC. International Journal of Mass Spectrometry. 2010 In press, doi:10.1016/j.ijms.2010.1009.1008.
95. Koizumi S, Yamamoto S, Hayasaka T, Konishi Y, Yamaguchi-Okada M, Goto-Inoue N, Sugiura Y, Setou M, Namba H. Neuroscience 2010;168:219–225. [PubMed: 20362643]
96. Guichardant M, Lagarde M. European Journal of Lipid Science and Technology 2009;111:75–82.
97. Nyadong L, Green MD, De Jesus VR, Newton PN, Fernandez FM. Analytical Chemistry 2007;79:2150–2157. [PubMed: 17269655]
98. Banos CE, Silva M. Journal of Chromatography A 2009;1216:6554–6559. [PubMed: 19691962]
99. Chi YG, Feng YL, Wen S, Lu HX, Yu ZQ, Zhang WB, Sheng GY, Fu JM. Talanta 2007;72:539–545. [PubMed: 19071652]
100. Kolliker S, Oehme M, Dye C. Analytical Chemistry 1998;70:1979–1985.
101. Zwiener C, Glauner T, Frimmel FH. Analytical and Bioanalytical Chemistry 2002;372:615–621. [PubMed: 11941429]

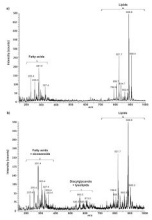

Figure 1.
Typical negative ion mode DESI mass spectra of a) normal rat spinal cord tissue and b) injured rat spinal cord tissue, using MeOH-water 50:50 (% v/v) as the solvent spray.

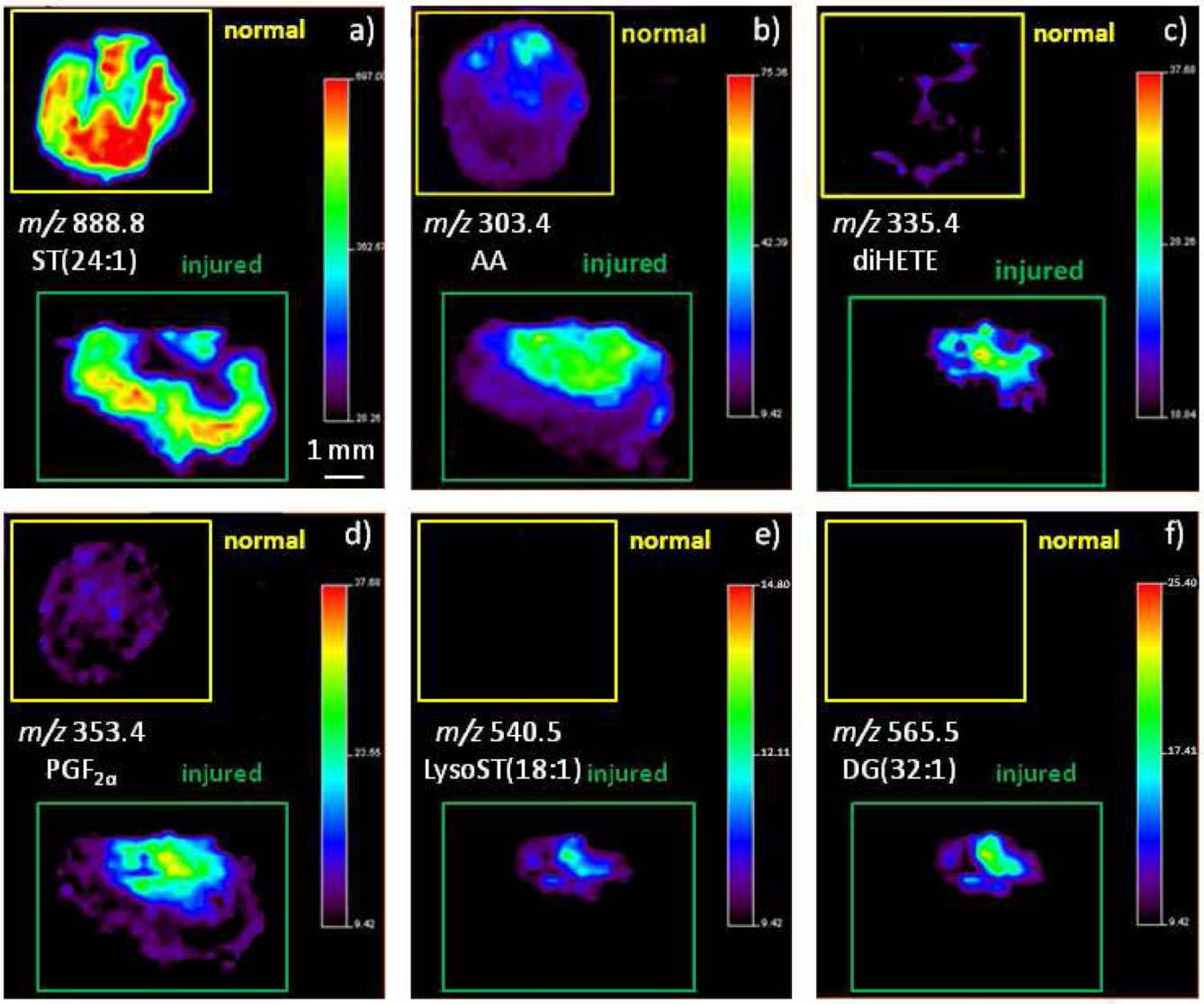

Figure 2.

Selected molecular ion $[M-H]^-$ images of specific lipids and fatty acids from analysis of rat spinal cord cross sections including normal and injured tissue, by DESI in the negative ion mode. Ion images of a) m/z 888.8 tentatively ST(24:1), b) m/z 304,4, tentatively AA, c) m/z 335.4, tentatively diHETE, d) m/z 353.4, tentatively $PGF_{2\alpha}$, e) m/z 540.5, tentatively LysoST(18:1) and f) m/z 565.5, tentatively DG(32:1).

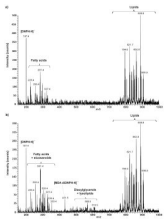

Figure 3.
Reactive DESI mass spectra in the negative ion mode of a) normal rat spinal cord tissue and b) injured rat spinal cord tissue, using a solvent of MeOH-water 50:50 (% v/v) doped with dinitrophenylhydrazine at 100 ppm.

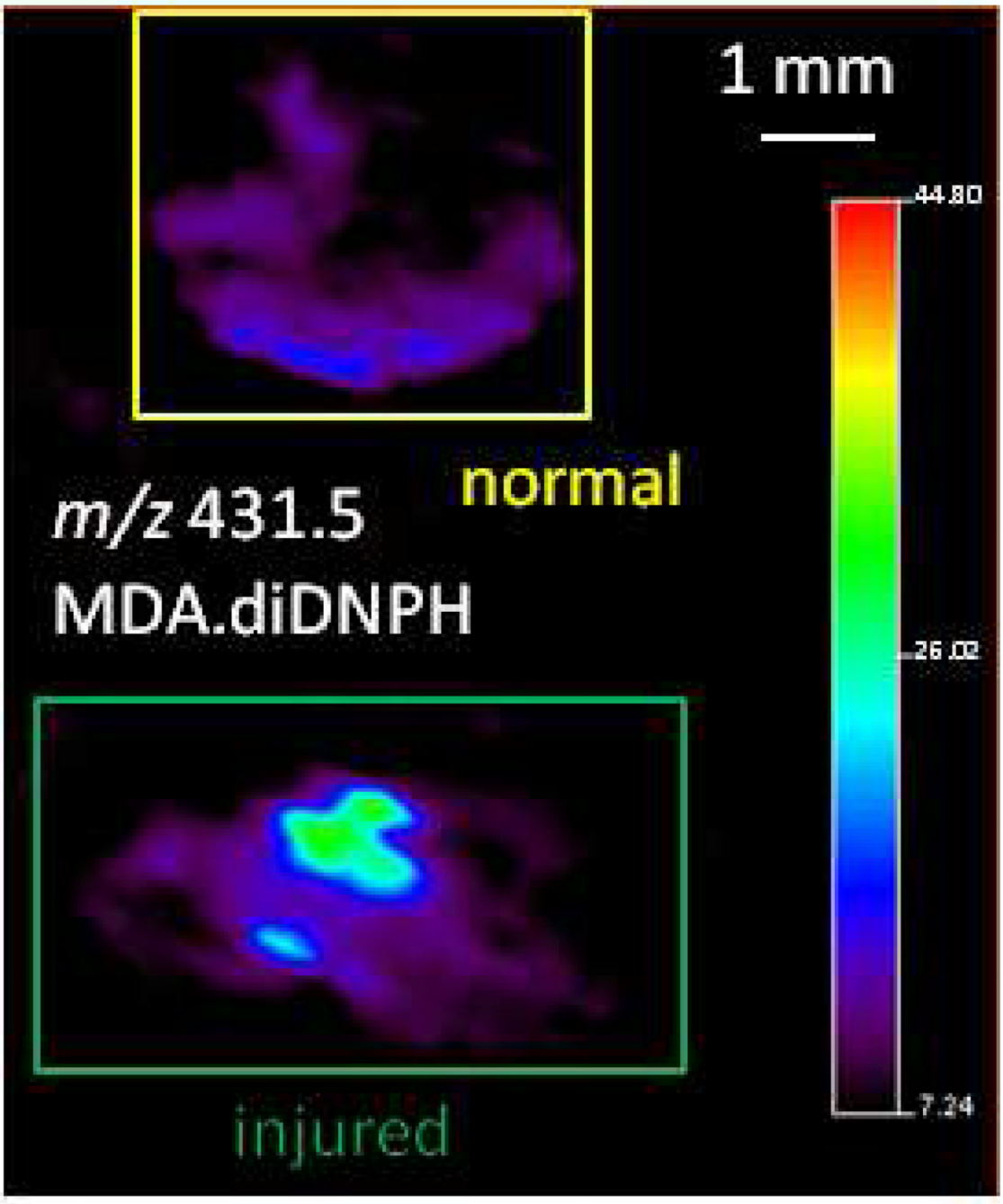

Figure 4.
Molecular ion $[M-H]^-$ image of the MDA.diDNPH from analysis of rat spinal cord cross sections including normal and injured tissue, by reactive DESI in the negative ion mode.

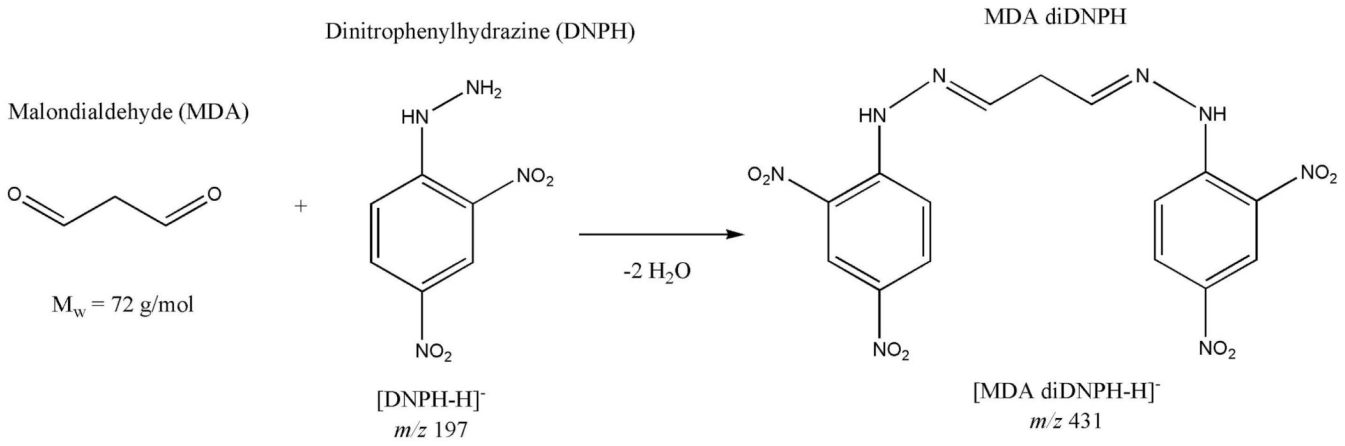

Scheme 1.

Table 1

Main new molecular species detected as deprotonated forms in injured rat spinal cord tissue in the negative ion mode

m/z	Molecular species[a]
303.4	Arachidonic acid (20:4)
335.4	5,15-diHETE
353.4	Prostaglandin $F_{2\alpha}$
537.5	LysoPG(18:1)
540.5	LysoST(18:1)
563.5	DG(32:2)
565.5	DG(32:1)
583.5	DG(34:2)
585.5	DG(34:3)
587.5	DG(34:4)
609.5	DG(36:7)
613.5	DG(36:5)

[a] All assignments are tentative, especially with respect to double bond location. See text